13th ewtec 2019 Proceedings of the 13th European Wave and Tidal Energy Conference 1-6 Sept 2019, Naples, Italy

Validation of simulated wave energy converter responses to focused waves for CCP-WSI Blind Test Series 2

Jennifer van Rij, Yi-Hsiang Yu, and Nathan Tom

Abstract—**Increasingly, focused waves are used as a design method to predict extreme loads for offshore structures, such as wave energy converters (WECs). However, the ability of computational methods to accurately simulate the prescribed focused waves and resulting wave structure interactions are not well-validated. As a participant in the Collaborative Computational Project in Wave Structure Interaction Blind Test Series 2, this study uses two computational fluid dynamics methods, WEC-Sim and STAR-CCM+, to evaluate three focused waves on two WEC-like bodies. WEC-Sim is a computationally efficient, midfidelity model based on linearized potential flow theory. STAR-CCM+ is a high-fidelity, three-dimensional, unsteady, Reynolds-averaged Navier-Stokes-based model. The two geometries considered are a hemispherical buoy and a cylindrical moon pool. The experimentally measured focused waves are reproduced in both codes, and the simulated displacements and mooring loads are obtained for each of the hydrodynamic bodies. The resulting STAR-CCM+ generated focused waves have approximately the same accuracy, in comparison to the analytic solution, as the experimentally generated focused waves. And, the WEC-Sim and STAR-CCM+ simulated displacements and mooring loads are, on average, within 5% of each other.**

Keywords—**Computational fluid dynamics, design wave, wave energy converter.**

I. Introduction

WAVE energy converter (WEC) design requirements, and consequently the cost of wave energy, are largely dictated by extreme wave loads [1]–[3]. Extreme waves, however, are a stochastic process. Stochastic, irregular wave loads are usually evaluated, experimentally or computationally, over a period of 3 hours, the typical timeframe required to obtain statistical convergence [4]. Although linear-based, numerical methods (e.g., WAMIT, WEC-Sim) have computation times that allow for such long timeframe evaluations, the assumption of linearity, and thus the accuracy of these evaluations, is highly questionable for large, extreme waves. Alternatively, high-fidelity computational fluid dynamics (CFD) simulations can accurately predict extreme, nonlinear wave loads, but are too computationally intensive to be practical for evaluating long-timeframe, irregular sea states [5], [6]. Given these computational constraints, the use of a "design wave," or focused wave, to predict extreme loads for offshore structures, such as WECs, is becoming increasingly common [7]–[10]. A focused wave is a linear sum of frequency components—amplitudes and phases—which may be formulated to give the most probable extreme wave or load, based on linear, broad-banded wave theory [11]. Using a focused wave is a deterministic, short timeframe (typically on the order of 60 s) means of evaluating the extreme loads for a stochastic sea environment. As such, the use of a focused wave saves computational and experimental evaluation time while, ideally, still accurately predicting the extreme design loads. However, in practice, the equivalence of focused waves to the stochastic extreme events that they are meant to represent, as well as the ability of computational methods to accurately simulate the prescribed focused waves and the resulting wave structure interactions, are not well-validated.

As a participant in the Collaborative Computational Project in Wave Structure Interaction (CCP-WCI) Blind Test Series 2 [12], this study uses two computational methods, WEC-Sim and STAR-CCM+, to evaluate three prescribed focused waves on two WEC-like bodies. WEC-Sim is a computationally efficient, midfidelity model based on linearized potential flow theory. STAR-CCM+ is a high-fidelity, three-dimensional, unsteady, Reynolds-averaged Navier-Stokes-(RANS) based CFD model. The two geometries considered are a hemispherical buoy and a cylindrical moon pool. The specified focused waves are reproduced in both codes, and the simulated displacements and mooring loads are obtained for each of

Paper ID number: 1483- Conference track: Wave hydrodynamic modelling

J. van Rij is with the National Renewable Energy Laboratory, 15013 Denver West Parkway, Golden, CO 80401, USA (e-mail: Jennifer.vanRij@nrel.gov).

Y.-H. Yu is with the National Renewable Energy Laboratory, 15013 Denver West Parkway, Golden, CO 80401, USA (e-mail: Yi-Hsiang.Yu@nrel.gov).

N. Tom is with the National Renewable Energy Laboratory, 15013 Denver West Parkway, Golden, CO 80401, USA (e-mail: Nathan.Tom@nrel.gov).

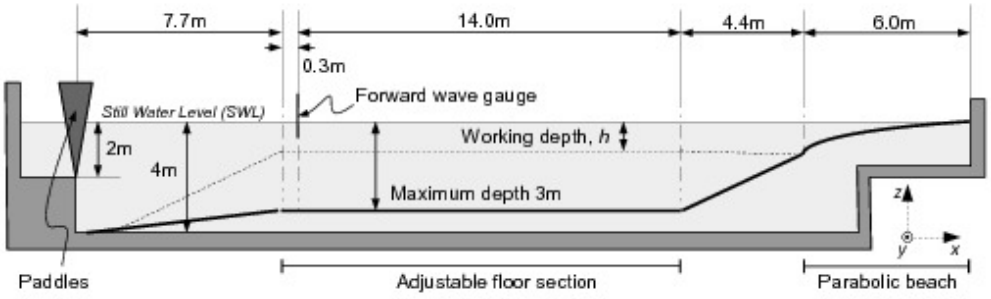

Fig. 1. COAST Laboratory Ocean Basin dimensions [12].

the hydrodynamic bodies. Results of the two methods are compared and verified in this study and will be validated against experimental data in future studies.

II. Experimental Parameters

This study is done in participation with the CCP-WSI Blind Test Series 2, which is funded by the Engineering and Physical Sciences Research Council of the United Kingdom, with the goal of bringing together the wave structure interaction community to share ideas and developments. As such, the experimental tank, WEC-like buoys, and wave parameters are reproduced as specified on the project website [12]. The experimental wave tank was the Plymouth University, United Kingdom, COAST Laboratory Ocean Basin, as illustrated in Fig. 1. The tank length is 35 m, the width is 15.5 m, and for these evaluations, a depth of h = 3 m was used, and the buoys were positioned at 14.8 m from the paddles. The two WEC-like buoys considered are a hemispherical buoy, as shown in Fig. 2, and a cylindrical moon pool, as shown in Fig. 3, where the dimensions and center of mass (CoM) are indicated. The specified mass, m, draft, and moments of inertia, I, for each geometry are provided in Table I. The mooring configuration for each buoy is a single linear spring that extends to the working depth, with a stiffness of 67 N/m.

TABLE I
BUOY PROPERTIES [12]

Geometry	m (kg)	Draft (m)	I_{xx} (kg·m²)	I_{yy} (kg·m²)	I_{zz} (kg·m²)
1	43.674	0.322	1.620	1.620	1.143
2	61.459	0.330	3.560	3.560	3.298

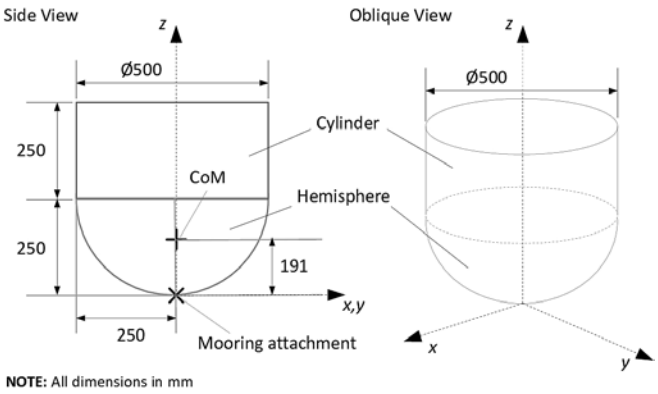

Fig. 2. Geometry 1: hemispherical buoy (dimensions in mm) [12].

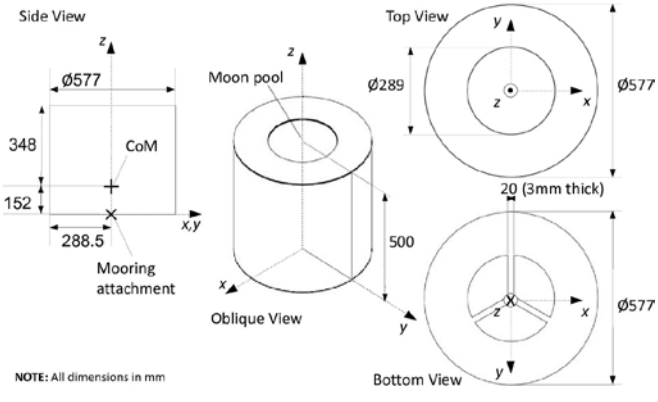

Fig. 3. Geometry 2: cylindrical moon pool (dimensions in mm) [12].

The focused waves in this study are obtained using NewWave theory [11], as given in (1) and (2), applied to a Pierson-Moskowitz spectrum, $S_n(\omega)$.

$$\eta(x,t) = \sum_{n=0}^{N} a_n \cos\left(k_n(x - x_f) - \omega_n(t - t_f)\right) \quad (1)$$

$$a_n = \frac{A_{cr} S_n(\omega) \Delta\omega_n}{\sum_{n=0}^{N} S_n(\omega) \Delta\omega_n} \quad (2)$$

Where, $\eta(x,t)$ is the surface elevation, N is the number of finite components, a_n is the component amplitude, x_f is the focus position, t_f is the focus time, k_n is the wavenumber, ω_n is the frequency, and A_{cr} is the total crest amplitude. Three focused waves are considered in this study, as specified in Table II. Where, f_p is the peak frequency, H_s is the significant wave height, and k_A is the total wave steepness. Using 244 wave components, with angular frequencies evenly spaced between 0.101563 Hz and 2 Hz, as was done in the experimental wave tank, the resulting theoretical focused wave surface elevations are plotted in Fig. 4.

TABLE II
WAVE PARAMETERS [12]

ID	A_n (m)	f_p (Hz)	H_S (m)	k_A (-)
1BT2	0.25	0.3578	0.274	0.128778
2BT2	0.25	0.4000	0.274	0.160972
3BT2	0.25	0.4382	0.274	0.193167

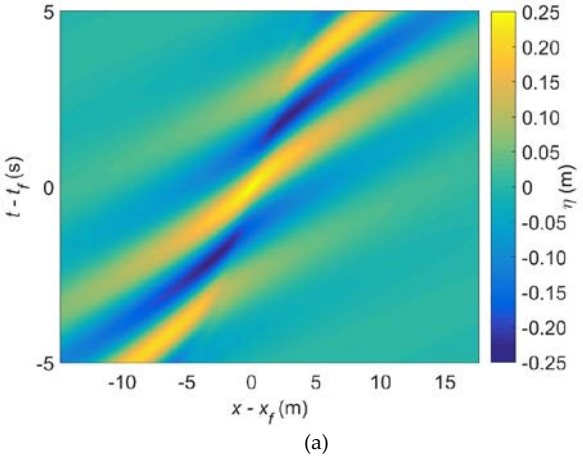

(a)

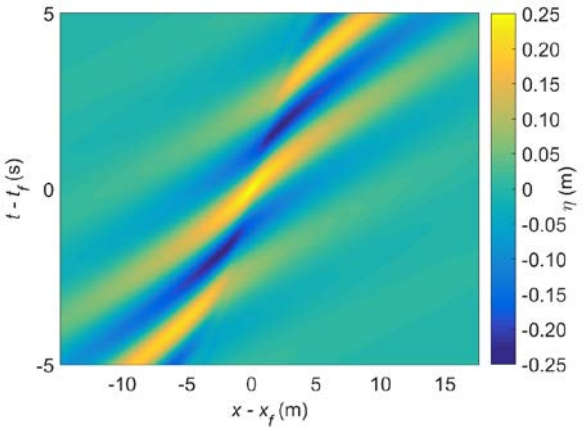

(b)

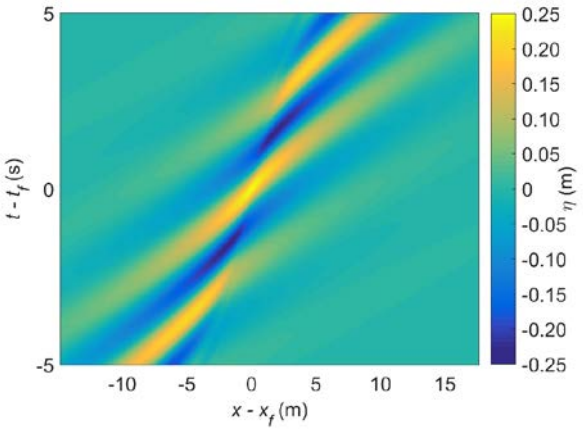

(c)

Fig. 4. Focused wave surface elevations: (a) 1BT2; (b) 2BT2; (c) 3BT2.

III. WEC-SIM MODELS

WEC-Sim is the midfidelity computationally efficient numerical model verified in this study. A detailed description of the theory and application of WEC-Sim is given on the WEC-Sim website [13]. However, the governing equation WEC-Sim solves to determine a WEC's system response in the time domain is Cummins' equation [14]. For a floating-body system, with its origin defined about its CoM, this equation of motion is given in (3).

$$(m + m_\infty)\ddot{x} = -\int_{-\infty}^{t} K(t-\tau)\dot{x}(\tau)d\tau + F_e - F_{hs} + F_v + F_{ext} \quad (3)$$

Where, m is the mass matrix, m_∞ is the added mass matrix at infinite frequency, x is the position vector, the term $\int_{-\infty}^{t} K(t-\tau)\dot{x}(\tau)d\tau$ is the convolution integral, representative of the resistive force on the body caused by wave radiation, K is the impulse response function, and, F_e , F_{hs} , F_v , and F_{ext} are the wave-excitation force, hydrostatic restoring force, viscous drag force, and external forces, respectively. The linear force coefficients m_∞, K, F_{hs}, and F_e are obtained using WAMIT models, as shown in Fig. 5, for the two geometries. By solving (3), WEC-Sim can simulate devices with six degrees of freedom (DOF) that are made up of rigid bodies, their

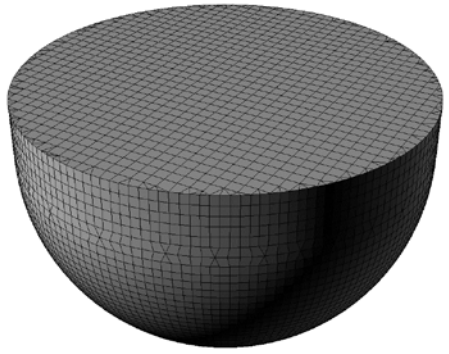

(a)

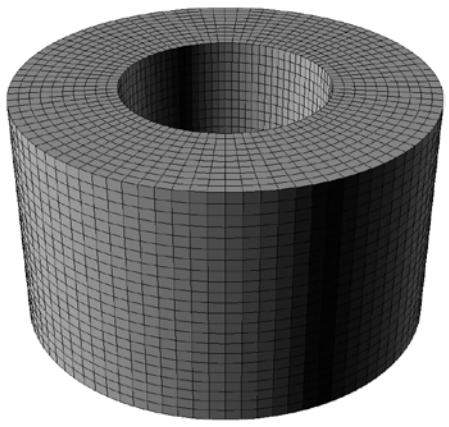

(b)

Fig. 5. WAMIT geometry and discretization for: (a) hemispherical buoy, 7945 panels, and (b) cylindrical moon pool, 6097 panels.

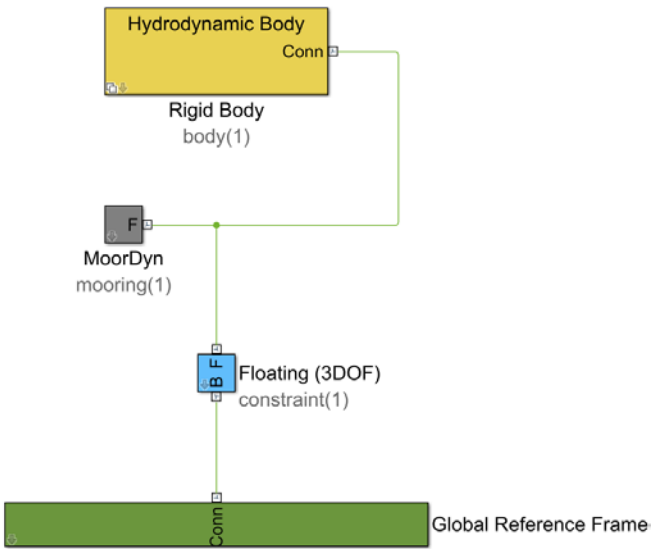

Fig. 6. WEC-Sim Simulink model.

constraints, simple power-take-off (PTO) mechanisms, and mooring systems.

A WEC-Sim model is comprised of a Simulink model and a MATLAB input file where the simulation and wave parameters, WAMIT hydrodynamic coefficients, mass properties, viscous drag coefficients, mooring stiffness, and PTO properties are specified. The Simulink model for the hemisphere and cylinder buoys, shown in Fig. 6, was created using prebuilt WEC-Sim blocks. The WEC-Sim block used to model the rigid bodies contains modules for calculating the wave radiation, excitation, hydrostatic restoring, viscous drag, and mooring forces, as specified in (3). In this Simulink model, the MoorDyn mooring block, rather than a simple spring matrix block [13], [15], is used to accurately model the taut mooring configuration. Where the specified stiffness and pretension force, as required to keep the floating body at the equilibrium position, is assigned within the MoorDyn input. The resting length of the spring is 2.215 m and 2.187 m, for the hemispherical buoy and cylindrical moon pool, respectively.

Besides the linear WAMIT hydrodynamic coefficients, WEC-Sim requires estimates of the viscous drag coefficients, C_D, for each body and DOF. These coefficients may be derived from experimental measurements, numerical simulations, or previously reported values. In this study, C_D are obtained by tuning the WEC-Sim response to the STAR-CCM+ response. By applying the CFD-generated wave elevations in WEC-Sim, C_D are adjusted to minimize the root-mean-square (RMS) error between the CFD- and WEC-Sim-predicted rigid body motions. The resulting C_D, for each geometry and focused wave, as applied in the subsequent studies, are reported in Table III.

TABLE III
WEC-SIM MODEL DRAG COEFFICIENTS AND REFERENCE AREAS

Geometry	Wave	A_x (m²)	$C_{D,x}$ (-)	A_z (m²)	$C_{D,z}$ (-)	A_θ (m⁵)	$C_{D,\theta}$ (-)
1	1BT2	0.134	0.8	0.196	1.1	5.563×10^{-4}	2.1
1	2BT2	0.134	0.8	0.196	0.8	5.563×10^{-4}	1.0
1	3BT2	0.134	0.6	0.196	0.4	5.563×10^{-4}	1.1
2	1BT2	0.190	0.4	0.204	0.9	8.553×10^{-4}	14.7
2	2BT2	0.190	0.2	0.204	0.6	8.553×10^{-4}	17.3
2	3BT2	0.190	0.4	0.204	1.0	8.553×10^{-4}	19.6

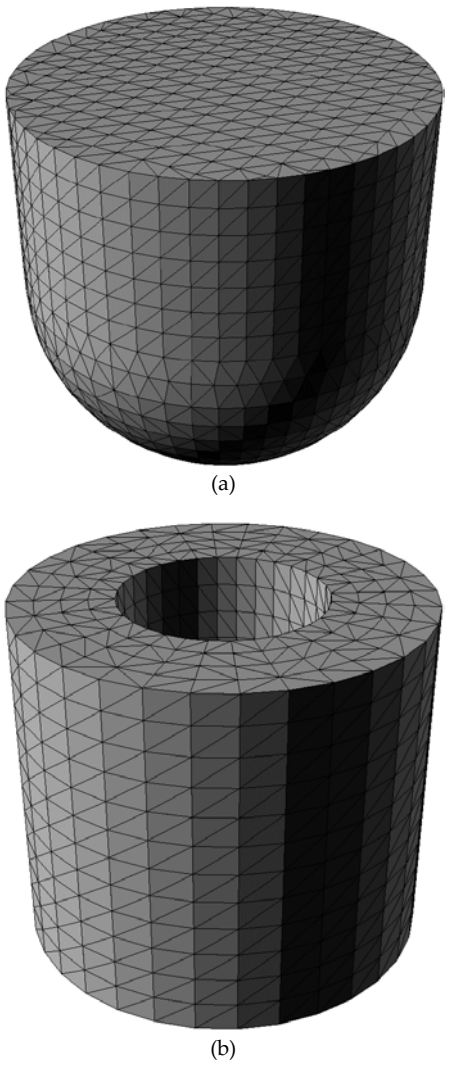

Fig. 7. Discretized surface for nonlinear buoyancy and Froude-Krylov pressure calculations in WEC-Sim: (a) hemispherical buoy, 2592 panels; (b) cylindrical moon pool, 2048 panels.

In addition to viscous drag forces, nonlinear restoring and Froude-Krylov forcing terms are also included in the WEC-Sim models. These weakly nonlinear forcing terms are calculated and integrated across the discretized body surfaces shown in Fig. 7 at each time step. Although the inclusion of nonlinear forces increases the computation time (~13 times longer for these cases), compared to wholly linear simulations, the accuracy of the resulting responses, in comparison to CFD, is significantly improved, particularly with drift forces accounted for, and the extra computational expense is considered worthwhile.

Using the described WEC-Sim model, time-varying wave forces may be applied, and the three-DOF equation of motion (e.g., surge, heave, and pitch) is solved for each WEC-like body in the time domain using a fourth-order Runge-Kutta time-marching algorithm to obtain the total system's dynamic response. The wave elevation in WEC-

Sim is specified, not calculated; as such, the wave elevation used in these studies could potentially be the analytic solution, the experimentally measured values, or the wave elevation values produced by CFD. For the solutions presented subsequently, the STAR-CCM+ generated NewWave elevations are used to better verify the models against each other. With these model inputs, WEC-Sim is run for each geometry and each of the three focused waves specified in Table II. A time step of dt = 0.0025 s is used and a total of 17.3 s is simulated, where the peak of the focused wave occurs at 10 s. Each of the simulations requires approximately 4 minutes to run.

IV. STAR-CCM+ MODELS

STAR-CCM+ [16] is used in this study for the high-fidelity CFD simulations. All the CFD simulations are run with an implicit, unsteady, three-dimensional, RANS model. For the turbulence closure model, the SST k-ω model, with "all y+ wall" treatment, is used. The free surface is modeled using the Eulerian multiphase, volume of fluid method, utilizing the fluid properties noted in Table IV. To accurately model the large-amplitude focused wave motions, as well as the mooring forces, using an acceptably sized grid, STAR-CCM+'s Dynamic Fluid Body Interaction (DFBI) overset method is used. The mooring line is modeled with a simple linear spring coupling with no repelling force.

The STAR-CCM+ computational-domain and grid-refinement zones are pictured in Fig. 8 for the hemispherical buoy (the cylindrical moon pool grid-refinement regions are the same). To be consistent with the experimental focused wave generation, the CFD-focused waves are also generated using 244 superposition waves, with equal $\Delta\omega_n$, and amplitudes and phases obtained from

TABLE IV
STAR-CCM+ MODEL FLUID PROPERTIES

Parameter	Setting	Unit
ρ_{water}	1000	kg/m^3
μ_{water}	1.155 x 10^{-3}	$Pa \cdot s$
ρ_{air}	1.184	kg/m^3
μ_{air}	1.855 x 10^{-5}	$Pa \cdot s$

(1) and (2). The computational domain is sized according to the experimental wave tank dimensions (pictured in Fig. 1). A velocity inlet boundary condition, with wave forcing, where the 244 superposition waves are applied, is specified at the channel inlet and side wall. Because STAR-CCM+, in the applied version (v13.02), cannot model both wave forcing and wave damping concurrently, the physical beach geometry is also simulated in CFD to minimize wave reflections at the outlet. Slip wall boundary conditions are specified at the top and bottom walls, and symmetry is utilized at the x-z plane.

The grid-refinement shown in Fig. 8 is obtained via mesh resolution and convergence studies, including those reported in [5], [7], [9], [10]. The grid-refinement zones are based on accurately modeling the wave propagation compared to the experimentally reported values, minimizing y+ on the the buoy surfaces, and sufficiently resolving the velocity gradients surrounding the model, while keeping the total number of cells at a minimum. For the results presented here, the grid resolution at the water surface is $\Delta z = 0.0125$ m ($H_s/\Delta z \approx 22$) in the vertical direction, $\Delta x = \Delta y/2 = 0.0125$ m ($\lambda_p/\Delta x \approx 800$) in the horizontal direction, and an average y^+ of 8.7 on the model surface. The average number of cells used for each of the validation simulations is 23.8 x 10^6. All the simulations are run for 15.3 s ($-10 \leq (t - t_f) \leq 5.3$ s), with t_f at 10 s, using second-order temporal accuracy, and time steps

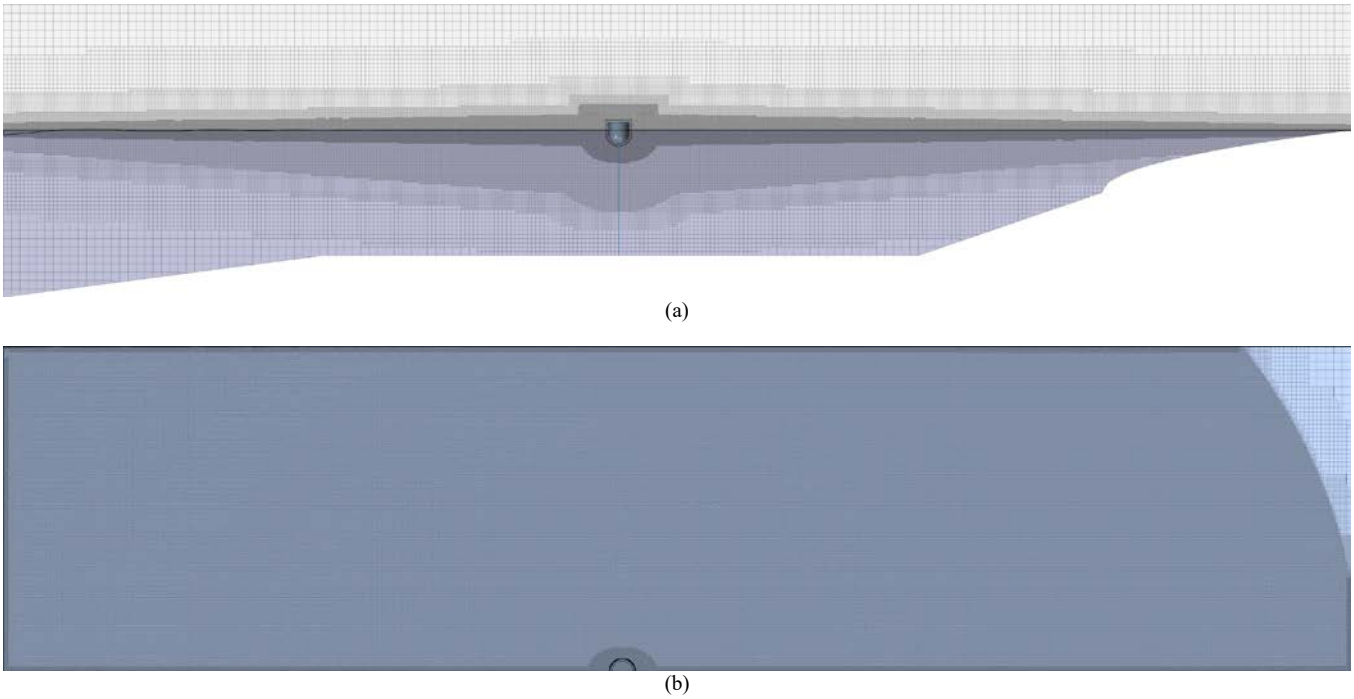

(a)

(b)

Fig. 8. STAR-CCM+ computational domain and grid-refinement zones for the hemisphere buoy: (a) side view and (b) top view.

TABLE V
EXPERIMENTAL AND STAR-CCM+ FOCUSED WAVE RMS ERROR RELATIVE TO THE ANALYTIC SOLUTION AT SELECT POINTS

		1BT2				2BT2				3BT2			
$(x - x_f)$	(m)	-4.25	-2.00	0.00	2.75	-4.25	-2.00	0.00	2.75	-4.25	-2.00	0.00	2.75
Experiment	(m)	0.0180	0.0125	0.0105	0.0098	0.0175	0.0127	0.0134	0.0114	0.0190	0.0116	0.0153	0.0150
STAR-CCM+	(m)	0.0122	0.0175	0.0204	0.0237	0.0104	0.0150	0.0169	0.0222	0.0103	0.0165	0.0186	0.0263

corresponding to a Courant number ($C = u\Delta t/\Delta z$) of 0.5 or less, to ensure numerical stability and accuracy. Where t_f in each case is the experimental focus wave time. Each of the three focused waves are simulated in an empty numerical wave tank, as well as with the hemispherical buoy or cylindrical moon pool, for a total of nine simulations. The simulations were run at the National Renewable Energy Laboratory's high-performance computing center. Each simulation required an average of 6 days to complete, and used ~55,000 cpu·hr.

V. RESULTS

WEC-Sim and STAR-CCM+ simulation results are presented and compared in Table V and VI and Figs. 9-11 for the time period, $-9.7 \leq (t - t_f) \leq 5.3$ s. In Figs. 9-11, the WEC-Sim and STAR-CCM+ time series results are shifted such that the numerically specified focus time aligns with the experimentally obtained focus time, which is at approximately 45 s.

Figure 9 shows the three NewWave surface elevations with time, as calculated analytically, experimentally measured, and simulated in STAR-CCM+ for positions relative to the focus position of -4.25, -2.00, 0.00, and 2.27 m. The STAR-CCM+ surface elevation results are for the empty numerical wave tank simulations. As stated previously, WEC-Sim does not model wave propagation; the WEC-Sim results presented here are obtained using the STAR-CCM+ generated wave elevations, and consequently, the WEC-Sim wave elevations are not plotted separately. The experimental and STAR-CCM+ focused wave elevation RMS error, relative to the analytic solution, is provided in Table V, for the same points as plotted in Fig. 9. The STAR-CCM+ generated focused waves have roughly the same accuracy at the focus position as the experimentally generated focused waves, in comparison to the analytic solution.

In Figs. 10 and 11, the STAR-CCM+ and WEC-Sim simulated displacements and mooring loads are plotted for the hemispherical buoy and the cylindrical moon pool, respectively. The STAR-CCM+ and WEC-Sim predicted maximum, preceding trough, and rise time for heave, surge, pitch, and the mooring force are tabulated and compared in Table VI. For these results, the pitch is considered positive in the counterclockwise direction. Generally, the overall first-order responses predicted by WEC-Sim and STAR-CCM+ compare well, where the displacement and mooring load parameters given in Table VI are within 4.7% of each other, on average. The average difference between the WEC-Sim and STAR-CCM+ parameters in Table VI for the hemispherical buoy is 3.6%, and for the cylindrical moon pool is 5.7%. The average difference between the WEC-Sim and STAR-CCM+ parameters in Table VI for the focused waves 1BT2, 2BT2, and 3BT2 is 3.4%, 4.0%, and 6.6%, respectively.

TABLE VI
CODE VERIFICATION PARAMETERS FOR WEC-SIM AND STAR-CCM+ SIMULATION RESULTS

			WEC-Sim						STAR-CCM+					
			11BT2	12BT2	13BT2	21BT2	22BT2	23BT2	11BT2	12BT2	13BT2	21BT2	22BT2	23BT2
Maximum	Heave	(m)	0.208	0.213	0.230	0.221	0.230	0.219	0.246	0.252	0.257	0.242	0.242	0.238
	Surge	(m)	0.373	0.394	0.425	0.369	0.381	0.402	0.373	0.393	0.446	0.411	0.453	0.510
	Pitch	(°)	17.391	22.096	25.954	16.152	16.784	16.579	15.015	20.415	25.329	13.802	14.371	13.965
	Mooring	(N)	46.815	47.362	48.844	46.388	47.127	46.654	48.082	48.583	49.258	49.892	50.197	50.426
Preceding trough	Heave	(m)	-0.178	-0.179	-0.181	-0.184	-0.181	-0.183	-0.164	-0.167	-0.172	-0.167	-0.170	-0.174
	Surge	(m)	-0.128	-0.117	-0.111	-0.101	-0.093	-0.087	-0.075	-0.074	-0.053	-0.057	-0.032	-0.009
	Pitch	(°)	-13.864	-18.924	-25.795	-14.752	-18.445	-21.035	-12.215	-17.274	-23.657	-13.368	-18.345	-24.202
	Mooring	(N)	19.756	19.687	19.556	19.565	19.765	19.678	20.422	20.256	19.978	22.055	21.941	21.706
Rise time	Heave	(s)	1.020	0.888	0.800	1.050	0.973	0.907	1.111	0.999	0.911	1.162	1.050	0.967
	Surge	(s)	1.110	1.048	1.020	1.153	1.103	1.087	1.128	1.074	1.055	1.203	1.143	1.136
	Pitch	(s)	0.813	0.797	0.770	0.980	0.950	0.950	0.780	0.726	0.692	0.943	0.919	0.922
	Mooring	(s)	1.028	0.885	0.785	1.055	0.970	0.913	1.111	0.990	0.889	1.166	1.053	0.965

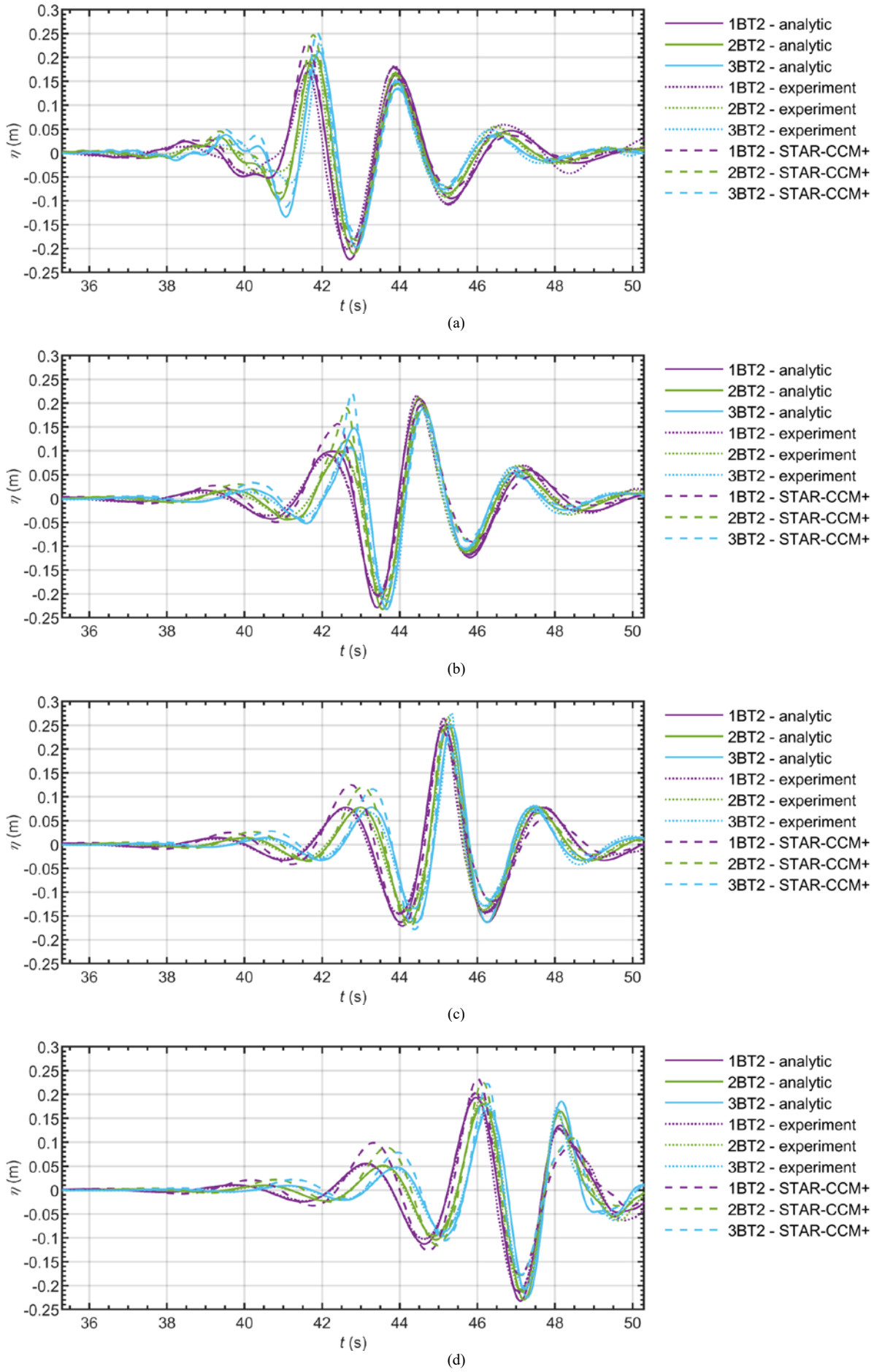

Fig. 9. Analytic, experiment, and STAR-CCM+ simulated 1BT2-, 2BT2-, and 3BT2-focused waves: (a) x-x_f = -4.25 m, (b) x-x_f = -2.00 m, (c) x-x_f = 0.00 m, and (d) x-x_f = 2.75 m.

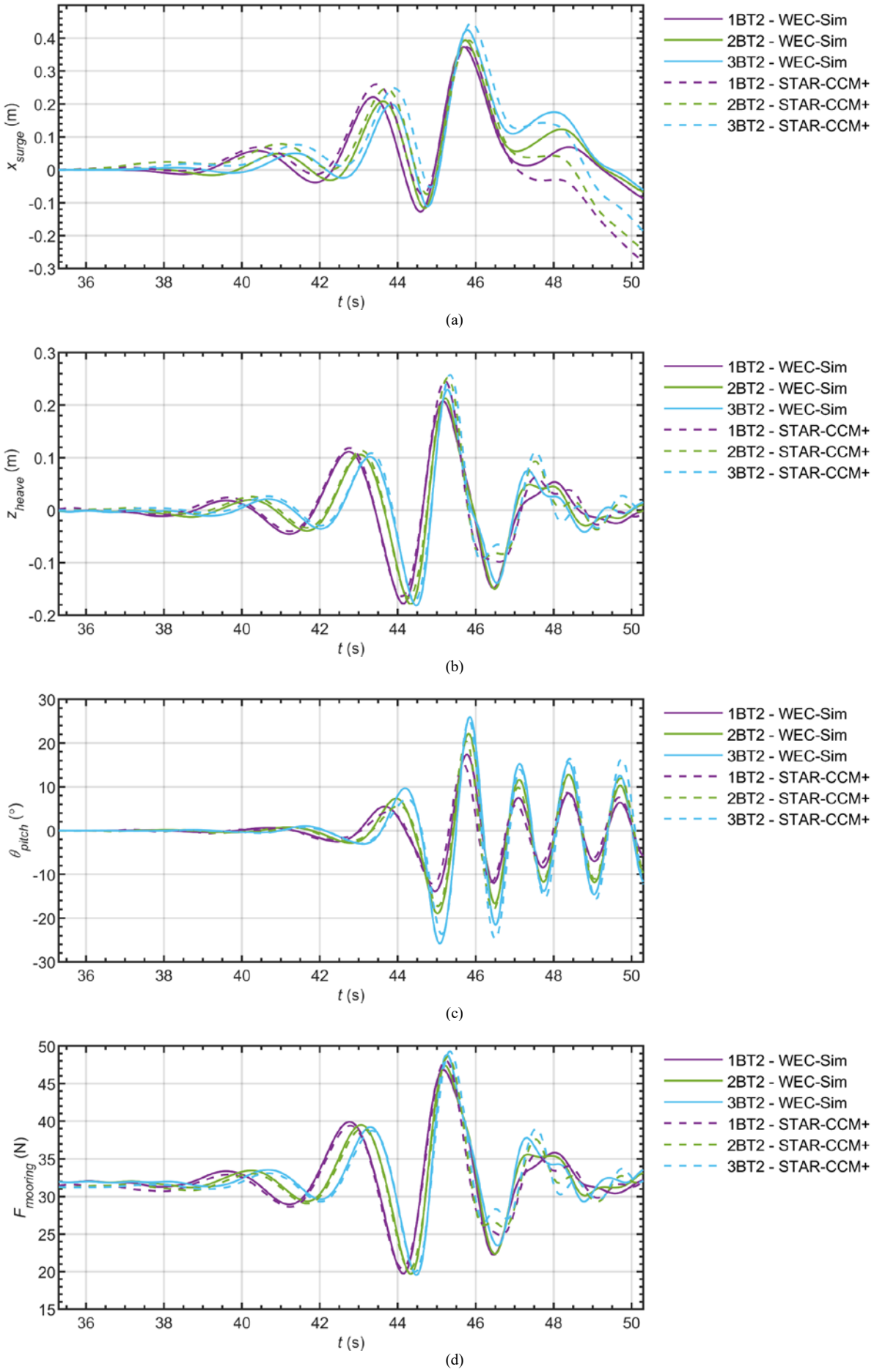

Fig. 10. WEC-Sim and STAR-CCM+ simulated responses for the hemispherical buoy to 1BT2-, 2BT2-, and 3BT2-focused waves: (a) surge, (b) heave, (c) pitch, and (d) mooring force.

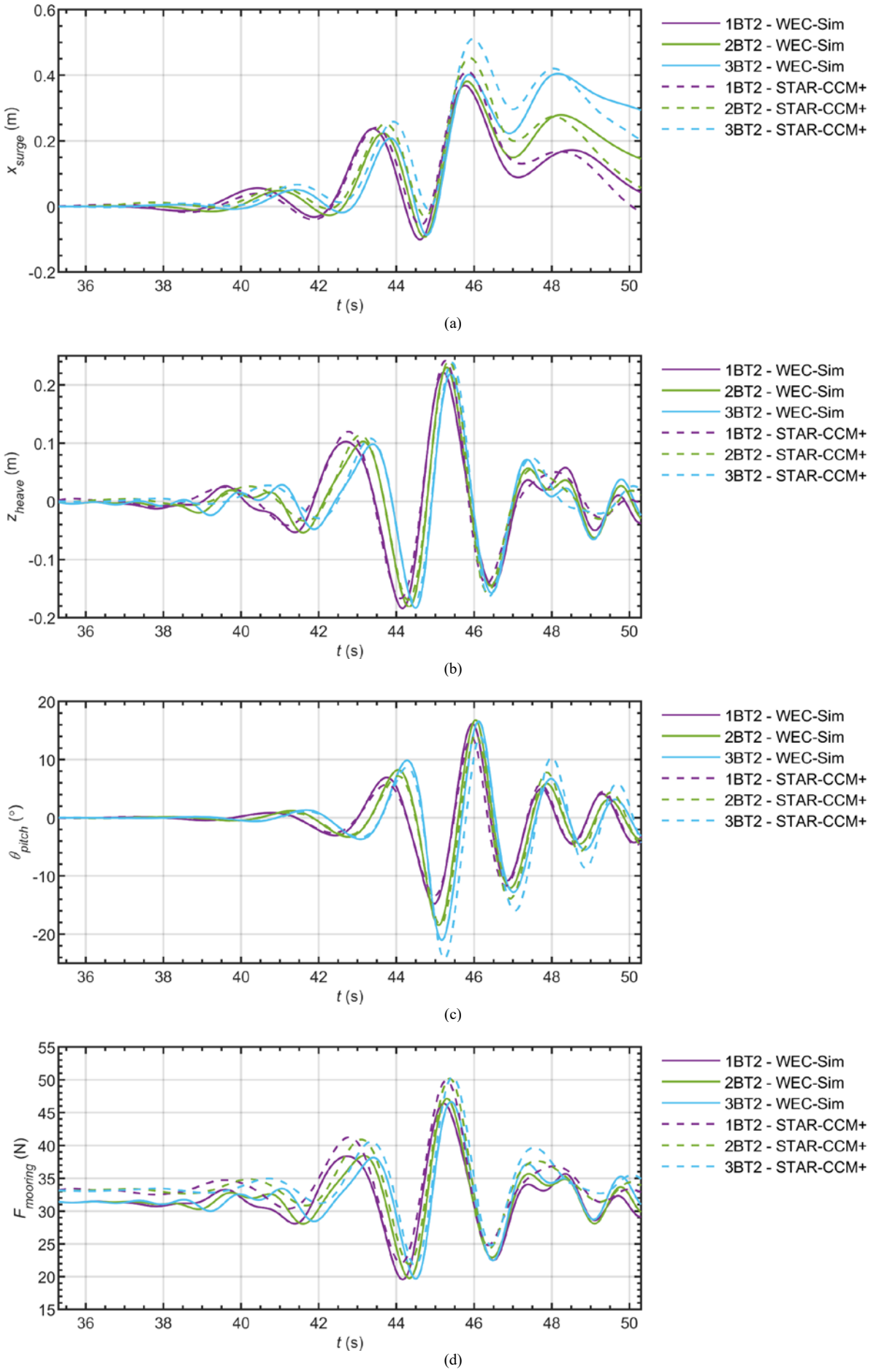

Fig. 11. WEC-Sim and STAR-CCM+ simulated responses for the cylindrical moon pool to 1BT2-, 2BT2-, and 3BT2-focused waves: (a) surge, (b) heave, (c) pitch, and (d) mooring force.

These results indicate that, as might be expected, WEC-Sim is less accurate than the high-fidelity CFD simulations, with the increasing nonlinearities associated with the internal water dynamics of the cylindrical moon pool and the steeper focused waves.

It should also be noted that the WEC-Sim data in Table VI will differ from that submitted to the CCP-WSI blind test series. In this study, for the purposes of code verification and C_D tuning, these WEC-Sim data are produced using the STAR-CCM+ generated wave elevations. However, for the comparative study, the WEC-Sim data will be produced using the experimentally measured wave elevations.

VI. Conclusion

Because of current computational limitations, the use of focused waves to design for extreme loads on offshore structures is becoming more commonplace. However, the ability of computational codes to accurately simulate focused waves and the resulting wave structure interactions is not yet well-validated. This study is presented as part of the wider CCP-WCI Blind Test Series, which is meant to verify and validate codes simulating focused-wave interactions with floating structures.

In the present study, two codes, WEC-Sim and STAR-CCM+, are used to simulate three different focused waves, with varying levels of steepness, and the subsequent response of two different wave energy converter (WEC)-like bodies. The two geometries evaluated are a hemispherical buoy and a cylindrical moon pool. The codes used are WEC-Sim, a linear-based computationally efficient code, and STAR-CCM+, a high-fidelity, more computationally intensive computational fluid dynamics code.

At this stage of the CCP-WCI Blind Test Series, only the experimentally measured surface elevations have been provided to the participants, not the floating structures' responses. However, based on these initial comparisons, the STAR-CCM+ generated focused waves have approximately the same accuracy, in comparison to the analytic solution, as the experimentally generated focused waves at the focus postion. And, the overall responses predicted by WEC-Sim and STAR-CCM+ compare well, where they are, on average, within 5% of each other, thereby verifying these models for use in future validation studies.

Acknowledgement

This work was authored by the National Renewable Energy Laboratory, operated by Alliance for Sustainable Energy, LLC, for the U.S. Department of Energy (DOE) under Contract No. DE-AC36-08GO28308. Funding provided by the U.S. Department of Energy Office Wind Energy Technologies Office. The views expressed in the article do not necessarily represent the views of the DOE or the U.S. Government. The U.S. Government retains, and the publisher, by accepting the article for publication, acknowledges that the U.S. Government retains a nonexclusive, paid-up, irrevocable, worldwide license to publish or reproduce the published form of this work, or allow others to do so, for U.S. Government purposes.

References

[1] The European Marine Energy Centre Ltd (EMEC), "Guidelines for Reliability, Maintainability and Survivability of Marine Energy Conversion Systems," 2009.

[2] V. S. Neary *et al.*, "Methodology for Design and Economic Analysis of Marine Energy Conversion (MEC) Technologies," Sandia National Laboratories (SNL), SAND2014-9040.

[3] D. S. Jenne, Y.-H. Yu, and V. Neary, "Levelized Cost of Energy Analysis of Marine and Hydrokinetic Reference Models," in *3rd Marine Energy Technology Symposium*, Washington, DC, United States, 2015.

[4] International Electrotechnical Commission, "Marine energy – Wave, tidal and other water current converters – Part 2: Design requirements for marine energy systems," IEC, Geneva, Switzerland, IEC TS 62600-2, 2016.

[5] van Rij, Jennifer, Yu, Yi-Hsiang, and Guo, Yi, "Structural Loads Analysis for Wave Energy Converters," in *Proceedings of the 36th International Conference on Ocean, Offshore & Arctic Engineering*, Trondheim, Norway, 2017.

[6] R. Coe, Y.-H. Yu, and J. van Rij, "A Survey of WEC Reliability, Survival and Design Practices," *Energies*, vol. 11, no. 1, p. 4, Dec. 2017.

[7] E. Quon, A. Platt, Y.-H. Yu, and M. Lawson, "Application of the Most Likely Extreme Response Method for Wave Energy Converters," in *35th International Conference on Ocean, Offshore and Arctic Engineering*, Busan, South Korea, 2016.

[8] E. J. Ransley, D. Greaves, A. Raby, D. Simmonds, and M. Hann, "Survivability of wave energy converters using CFD," *Renew. Energy*, vol. 109, no. Supplement C, pp. 235–247, Aug. 2017.

[9] van Rij, Jennifer, Yu, Yi-Hsiang, and R. G. Coe, "Design Load Analysis for Wave Energy Converters," in *Proceedings of the 37th International Conference on Ocean, Offshore & Arctic Engineering*, Madrid, Spain, 2018.

[10] R. G. Coe *et al.*, "CFD design load analysis of a two-body wave energy converter," *J. Ocean Eng. Mar. Energy*, 2019.

[11] P. S. Tromans, A. R. Anaturk, and P. Hagemeijer, "A new model for the kinematics of large ocean waves - application as a design wave," in *The 1st International Offshore and Polar Engineering Conference*, Edinburgh, UK, 1991.

[12] "CCP-WSI blind test series 2." [Online]. Available: https://www.ccp-wsi.ac.uk/blind_test_series_2.

[13] "WEC-Sim." [Online]. Available: https://wec-sim.github.io/WEC-Sim/.

[14] W. E. Cummins, "The Impulse Response Function and Ship Motions," Department of the Navy, David Taylor Model Basin, Oct. 1962.

[15] M. Hall, "MoorDyn User's Guide," Department of Mechanical Engineering, University of Maine, Dec. 2015.

[16] "STAR-CCM+." [Online]. Available: http://mdx.plm.automation.siemens.com/star-ccm-plus.